

# Development of a Holographic Particle Diagnostic System and Its Application to Measurements of Spray Characteristics

**Y. J. Choo**

*Korea Atomic Energy Research Institute,  
105, Yuseong-Gu, Daejeon 305-600, Korea*

**B. S. Kang\***

*Department of Mechanical Engineering, Chonnam National University,  
300, Yongbong-Dong, Buk-Gu, Gwangju 500-757, Korea*

Particle diagnostics involving three dimensional distributions are important topics in many engineering fields. The holographic system is a promising optical tool for measuring three dimensional features of particles. In this study, we developed a holographic particle diagnostic system with diffused illumination to measure the sizes and 3-D velocities of moving particles using automatic image processing. First, basic optical systems for pulse laser recording, continuous laser reconstruction, and image acquisition were constructed. One of inherent limitations of particle holography is its long depth of focus in particle images, which causes considerable difficulty in determination of particle positions in the optical axis. To solve this problem, three new auto-focusing parameters (AFPs) corresponding to particle sizes were introduced. The developed system was applied to spray droplets to validate its capabilities. Three dimensional positions of particles viewed from two sides were decided using AFPs and then three dimensional particle velocities were extracted using a particle tracking algorithm. Comparison of measured sizes and three dimensional velocities of particles with those obtained using a laser instrument, PDPA (Phase Doppler Particle Analyzer), showed that the developed holographic system produced consistent results.

**Key Words :** Holographic Particle Diagnostic System, Diffused Illumination Holography, Particle Tracking, Focusing Parameter, 3D Particle Position

## Nomenclature

$D$  : Particle diameter  
 $E$  : Position error of particle  
 $R$  : Moving distance of particle  
 $\Delta t$  : Laser pulse interval  
 $u$  : Uncertainty  
 $V$  : Particle velocity  
 $X, Y$  :  $x$  and  $y$  axis  
 $Z$  :  $z$  axis (optical axis)

## Subscripts

$I$  : CCD sensor  
 $p$  : Reconstructed particle

## 1. Introduction

The particle flow fields encountered in many engineering areas have many complexities and irregularities, and a three dimensional nature. To investigate the characteristics of such particle flow fields, various measurement techniques and instruments have been developed and commercialized. Among these, non-intrusive optical instruments, such as Imaging, LDV (Laser Doppler Velocimetry), PDPA (Phase Doppler Particle Analyzer), PIV (Particle Image Velocimetry), have

\* Corresponding Author,

**E-mail :** bskang@chonnam.ac.kr

**TEL :** +82-62-530-1683; **FAX :** +82-62-

Department of Mechanical Engineering, Chonnam National University, 300, Yongbong-Dong, Buk-Gu, Gwangju 500-757, Korea. (Manuscript Received May 8, 2006;

Revised October 20, 2006)

advanced remarkably, because of rapid laser, imaging system, and computer developments. However, a measurement tool capable of determining 3-D features of particles over a complete test volume as a function of time remains on the developmental wish-list. In recent years, much experimental efforts have been made to try to overcome limitations of 2-D measurements, for example, stereoscopic PIV system for 3-D velocity measurements. From this point of view, a holographic method probably offers the ultimate solution, because of its superiority at realizing 3-D fields in itself. However, many problems must be overcome, and holographic systems very much remain at the developmental level.

As for spray diagnostic systems, considerable progress made in laser instrument technologies like PDPA, which now makes it possible to obtain reliable data on droplet sizes and velocities in dilute spray regions. However, these methods are inherently limited in dense spray regions, where liquid elements are rather large and non-spherical. In addition, no information on spray structure can be provided by this kind of instrument. On the other hand, the holographic technique reproduces the frozen spray as a 3-D image, from which droplet sizes and position, 3-D velocities and spray structures can be investigated.

From early years, the holographic technique obtained great interests of researchers owing to methodological possibilities of particle diagnostics and 3-D flow measurements (Vikram, 1979). The holographic system for 3-D flow field measurements is Holographic PIV, which extends the correlation technique used in 2-D PIV to three dimensions. HPIV has been improved remarkably to satisfy strong demands of 3-D features (Barnhart, 2001). Like conventional PIV, HPIV concerns only about flow fields using scattered spots by particles. On the other hand, the holographic system for particle diagnostics can measure the shapes, sizes, velocities, and 3-D positions of individual particles which are important parameters in many particle fields. Unlike HPIV, few works related to particle diagnostics have been conducted so far in the limited range (Hausmann and Lauterborn, 1980; Kang, 1995; Feldmann et al., 1999).

Hausmann and Lauterborn (1980) measured gas bubbles in water using the automated digital image processing system. The focusing parameter using the differential filter was introduced. However, they concluded that primary limitation was imposed by low spatial resolution of image device (roughly  $38 \mu\text{m}$ ) and long calculation time. Feldmann (1999) obtained more successful and quantitative results for the moving bubbles and spray droplets. They measured the 3-D positions of particles using stereo-matching of particle images reconstructed in two sides. However, he didn't attempt to compensate geometry distortion made by wavelength difference between recording and reconstruction stages. Kang (1995) used a two-reference-beam double-pulse technique, which featured switching the polarization of the laser light between pulses to separate the first and second droplet images, thus avoiding the overlapping problem and the directional ambiguity of particle movement. The method developed was applied to fan-shaped sprays formed by two impinging high-speed jets.

In the present study, a diffused illumination holographic system was developed to measure the sizes and 3-D velocities of moving particles using automatic image processing. Initially, basic optical systems for pulse laser recording, reconstruction with a continuous laser having a same wavelength with the pulse laser, and image acquisition were constructed. One of inherent limitations of particle holography using forward scattered light is its long depth of focus in particle images. This characteristic causes considerable difficulty in determination of particle positions in the optical axis, and prevents full automation of holographic image processing from image capture to particle characterization in space and time. To solve this problem, three auto-focusing parameters (AFPs) corresponding to particle sizes were introduced and verified by present authors (2006). The developed holographic velocimetry system was applied to real spray droplets to validate its capabilities. Three dimensional positions of particles viewed from two orthogonal sides were decided using AFPs, and then three dimensional particle velocities were extracted using a particle tracking algorithm. Measured sizes and three dimensional

velocities of particles were compared with those obtained using a laser instrument, PDPA.

## 2. Hologram Recording and Reconstruction

To obtain the velocity of a particle, position information of the particle is required at two moments in time, and double pulse recording in one direction is usually used to perform this. However, the quality of reconstructed images is poorer on doubly exposed film, and it is difficult to distinguish particles in each pulse. To avoid these drawbacks, we constructed an orthogonal double pulse holographic system in two normal directions, as shown in Fig. 1. In this system, two recording systems are positioned orthogonally and each hologram is exposed once to record a particle at one moment in time. One point that should be considered carefully in this recording system arrangement is the matching of coordinates in each direction, which will be discussed in detail

in the section 3.

Each recording system is a typical off-axis holographic system. The light source was a twin Nd-YAG laser (Brilliant B, Quantel), which generated a wavelength of 532 nm, vertically polarized, 300 mJ output energy laser beams of frequency 10 Hz. An injection-seeder was used to increase the coherence length of the output laser to more than one meter for the holographic application. The pulse interval between two lasers was controllable from 1 to 900  $\mu$ s, and the short pulse duration (10 ns) used assured the freezing of all moving particles and the clarity of the resulting images. The light from the laser was separated using a beam splitter, which divided the beam into reference and object beams. The object beam was expanded and collimated to a diameter of 10 cm using a Galilean type of beam expander. This plane wave was passed through the test section and finally was intercepted at a  $10.16 \times 12.7$  cm<sup>2</sup> holographic glass plate. The beam intensity was adjusted using an attenuator to achieve a reference-to-object beam intensity ratio of approximately 4 to 1, which was selected by trial-and-error. A diffuser was positioned before the test section to provide a uniform background and to decrease the depth of focus in particle images. The path length difference between the object and reference beams was minimized to guarantee satisfactory interference between two beams irrespective of the coherence length of the laser. The holographic plate was positioned orthogonally to the plane bisecting the reference and object beams to reduce astigmatism.

Water spray droplets produced by a commercial full cone spray nozzle with a 1.0 mm orifice were used as a recording target and their sizes and velocities were measured. A high-pressure N<sub>2</sub> cylinder with a pressure regulator was used to pressurize a liquid reservoir so as to direct a non-fluctuating stable liquid flow to the spray nozzle. Water was injected at injection pressures of 147, 196, and 294 kPa to produce droplets within any range where our system can resolve.

The recorded holograms were developed, fixed, and dried as for photographic film processing, and then reconstructed and analyzed using an image processing system. To avoid image aberrations

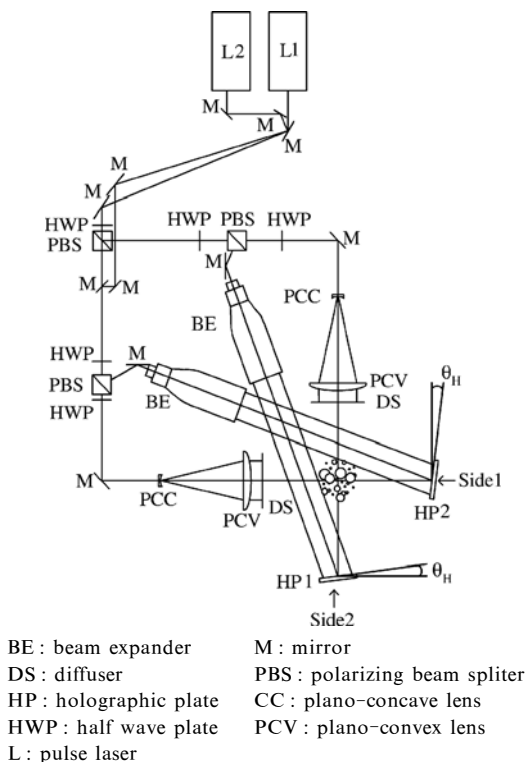


Fig. 1 Holographic recording system

tions, the optical system used for recording was also used for the reconstruction process. The light source used for the reconstruction process was a diode pumped crystal laser (CrystaLaser Co.), which generated the same wavelength of 532 nm as recording, vertically polarized, and 500 mW output laser beams. No lens was used for the digital CCD camera (Kodak Co., MegaPlus ES 1.0,  $1,008 \times 1,018$  pixels,  $9 \mu\text{m}$  pixel size) to exclude the extension of depth of focus by camera lens, and to obtain as wide an angular aperture as possible. The camera was moved automatically using a three-axis translation stage (PI Inc.) and positioned with a resolution of 33 nm.

The coordinates of the recording and reconstruction systems with the origin at the center of the hologram, are shown in Fig. 2. The object beam was directed along the  $Z$  axis normally to the  $X$ - $Y$  plane. During recording, the diffuser and test section are in the left space ( $-Z$  axis) of the holographic film. Instead of reconstructing virtual images, real particle images were reconstructed in the right space ( $+Z$  axis) of the hologram using a conjugate reference beam obtained by rotating the hologram by  $180^\circ$  with respect to the  $Y$  axis. The plane in which the camera sensor was located was defined as the image plane, and the coordinates of sensor pixels were defined as  $(x_I, y_I, z_I)$ . The image of one particle with its speckle background was defined as a Region of Interest (ROI). The predicted coordinate of a focused particle was defined as  $(x_p, y_p, z_p)$ .

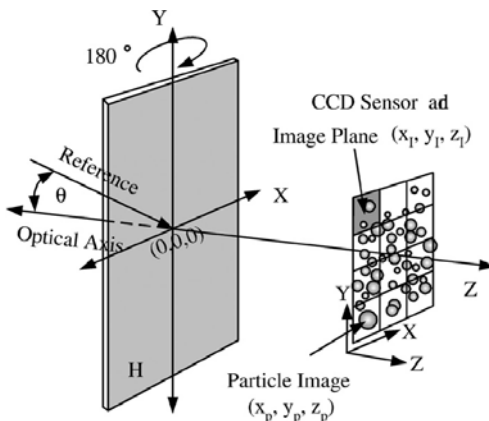


Fig. 2 Coordinates of the reconstruction system

Reconstructed images can be analyzed in real-time or after acquiring all images. In this study, the latter method was used to avoid long instrument operation times required for real-time analysis. Thus, all reconstructed images were first captured by moving the camera in equal increment along the optical axis. To do this, an adequate increment of camera movement should be predetermined because the minimum resolution of image analysis along the optical axis is determined by this pre-set increment, as does the effectiveness of the image analysis. Considering the depth of field of the smallest particle, the camera increment was set at  $33 \mu\text{m}$ , which was 1,000 times the minimum resolution of the translation stage.

### 3. Algorithms for Particle Image Processing

The most important prerequisite required to precisely determine particle velocities is an adequate focusing parameter, which is used to determine the particle positions along an optical axis. To facilitate this, present authors (2006) investigated the characteristics of the particle position along an optical axis in particle holography. The characteristics of speckles and particle images versus hologram aperture and particle positions along the optical axis were investigated. Three auto-focusing parameters corresponding to the sizes of particles to determine the focal plane occupied by particles along the optical axis were introduced and verified. More details are not discussed here for brevity but some important points will be introduced here for the sake of understanding.

#### 3.1 Particle size determination

It is important to define an appropriate image processing procedure for measuring particle size, regardless of particle size and image contrast, because compared with large particles, relatively small particles possess low image contrast and they are affected substantially more by speckles. Validation of the measuring procedure for the particle size was conducted using a transparent screen of dark dots as a substitute of real droplets for convenience and to aid systematic investigation. The

screen was a kind of reticle manufactured with high accuracy and resolution for calibration purpose of optical systems and it contains various dot sizes ranging from 8 to 300  $\mu\text{m}$ .

Figure 3 describes the image processing procedure to determine particle sizes. Figure 3(a) is the original image of a 300  $\mu\text{m}$  particle. To remove speckle noise, a wavelet technique (Gonzalez et al., 2004) was used; Fig. 3(b) represents the image after this treatment. The gray level of image Fig. 3(b) is transformed to obtain a gray level distribution between 0 and 1. This transformation was applied to obtain consistent particle size measures independent of the recording and reconstruction conditions used. Figure 3(c) shows the final image binarized using appropriate criteria; this binarized image was used to determine particle size. The size of a particle was obtained by evaluating the equivalent diameter of a particle from the total area of particle image. The binarization cri-

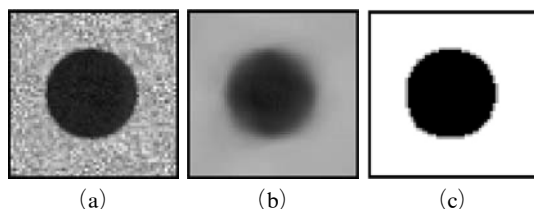


**Fig. 3** Image processing procedure for determination of particle size; (a) original image, (b) Wavelet transform, (c) binarization

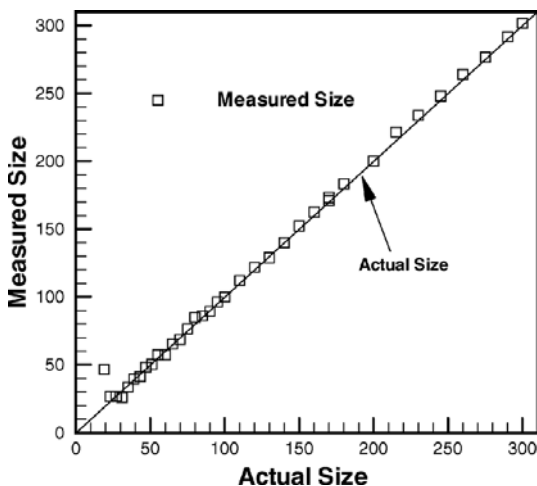


**Fig. 4** Size calibration results

teria of normalized gray value (0.637 in the present experiment), was decided based on considerations of size measurement consistency during the calibration procedure, which is shown in Fig. 4. The final size measurements obtained, shown as symbols, agree well with the real sizes shown as a solid line. For particles below 20  $\mu\text{m}$ , error is inevitable because the corresponding number of pixels is only one or two. Therefore, a size of 20  $\mu\text{m}$  was assigned to all particles with a diameter  $< 20 \mu\text{m}$ .

### 3.2 Particle position determination

Three auto-focusing parameters introduced by present authors (2006) are the Correlation Coefficient, the Sharpness Index, and the Depth Intensity. The Correlation Coefficient Method (CCM) uses a correlation coefficient between two sectional images of one particle along the optical axis. The correlation coefficient can be approximated using Gaussian curve fitting, and the center of the curve can be taken to represent the focal plane of a particle. The Sharpness Index Method (SIM) uses a cumulative histogram of particle image containing the speckle background. The cumulative histogram has a linear region connecting the region for background and that for particle. The slope of this linear region represents boundary sharpness so it can be used as a focusing parameter.

The Depth Intensity Method (DIM) uses a simple concept that the focal image of a particle would show the darkest intensity at the center of a particle. The depth intensity distribution can be obtained if the gray value of the cross-section images of a particle is plotted along the optical axis. This distribution has the lowest value at the focal plane of a particle because the gray value of a particle center increases as the distance from the focal plane increases. This method was specially introduced for relatively small particles (below 50  $\mu\text{m}$ ).

The three focusing parameters introduced above respond differently to particle size. Therefore, appropriate focusing parameters corresponding to the particle sizes were determined; 1) Large size particles ( $D > 300 \mu\text{m}$ ): CCM and then SIM, 2) Medium size particles ( $50 \mu\text{m} < D < 300 \mu\text{m}$ ): CCM,

3) Small size particles ( $D < 50 \mu\text{m}$ ): DIM. To validate the above focusing parameters, a plane image of a dot array screen containing equally spaced dots ( $500 \mu\text{m}$  size) in two directions was recorded and the positions of each dot along the optical axis were evaluated. Reconstructed axial positions of dots on the screen at  $z=322 \text{ mm}$  from the hologram were calculated by CCM or SIM as shown in Fig. 5. The uncertainty of the CCM is  $u_z = \pm 44.74 \mu\text{m}$  and that of the SIM is  $u_z = \pm 16.07 \mu\text{m}$  (about 1/3 of CCM). Therefore, the SIM produces a better prediction of axial position than the CCM.

More accurate prediction of axial positions for relatively large particles is possible by the successive application of the CCM and the SIM. Specifically, the approximate focal plane of a particle is determined first by applying the CCM and then the SIM is used to determine the focal plane ac-

curately using the reduced width of particle images. The results of the successive applications of the CCM and the SIM to particle images on the screen located at different axial position from the hologram are shown in Table 1. The total error,  $E$ , is defined as the difference between the predicted and real positions of a particle. The magnitude of errors in the  $x$  or  $y$  axis is negligible compared with physical size of a CCD pixel ( $9 \mu\text{m}$ ). For the  $z$  axis, the average value of uncertainties is  $\pm 19.4 \mu\text{m}$ , which is really small value of error considering a few millimeter order of depth of field in normal holography.

### 3.3 Coordinate matching

As discussed in the section 2, double pulse holographic recording system in two normal directions is used in the present study to enhance image quality and to avoid confusion between pulses. However, the coordinates in each direction should be matched carefully. A simple experiment to correct the coordinates was conducted initially to solve this problem. Specifically, a single pulse hologram in both two normal directions was recorded. Figure 6 shows the typical single pulse image of spray droplets, which were holographically recorded and then reconstructed in two normal directions. The images of side 1 and 2 were taken at the center of spray axis in the  $x$  and  $z$  directions, respectively. Then a coordinate transformation matrix, which reflected all involved errors such as translation, rotation, and scaling, was

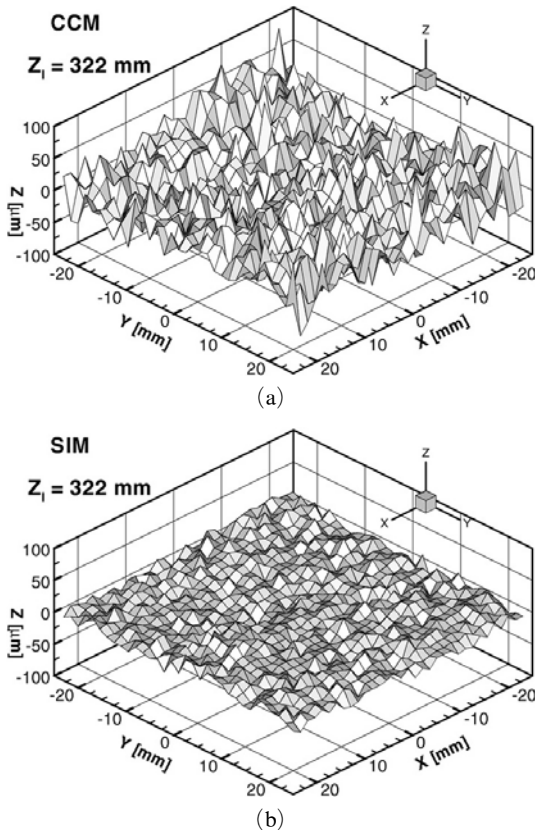


**Fig. 5** Reconstructed positions of particles ;  
(a) CCM, (b) SIM

**Table 1** Means and uncertainties of particle positions

$z_p$ [mm]	$\bar{E}_x \pm u_x$ [ $\mu\text{m}$ ]	$\bar{E}_y \pm u_y$ [ $\mu\text{m}$ ]	$\bar{E}_z \pm u_z$ [ $\mu\text{m}$ ]
170	$2.146 \pm 16.07$	$10.725 \pm 10.47$	$0 \pm 22.85$
208	$3.418 \pm 14.73$	$7.569 \pm 11.53$	$0 \pm 25.84$
246	$-4.733 \pm 15.04$	$11.311 \pm 10.07$	$0 \pm 19.70$
284	$3.828 \pm 15.10$	$8.687 \pm 9.66$	$0 \pm 13.47$
322	$0.153 \pm 15.44$	$11.814 \pm 10.25$	$0 \pm 16.07$
360	$1.699 \pm 15.76$	$6.031 \pm 10.50$	$0 \pm 15.68$
398	$-0.935 \pm 15.39$	$6.154 \pm 11.81$	$0 \pm 19.08$
440	$-4.239 \pm 18.04$	$-6.697 \pm 11.47$	$0 \pm 30.36$
Total	$0.796 \pm 16.28$	$8.899 \pm 11.51$	$0 \pm 19.37$

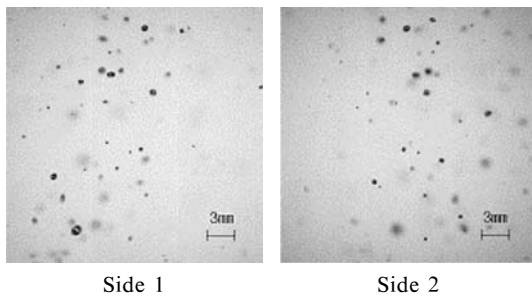


**Fig. 6** Typical reconstructed images of droplets captured from two normal sides

constructed. Once this transformation matrix was obtained, it was used later to match the coordinates in each direction for double pulse hologram in two normal directions.

## 4. Application to Spray Droplets

### 4.1 Procedure for image analysis

The developed image processing algorithms for the determination of three dimensional coordinates of particles were applied to determine three dimensional spray droplet velocities. The flow chart of the full procedure from the recording of this type of hologram to the final extraction of three dimensional velocities is shown in Fig. 7. The procedure consists of three stages. In the first stage, double pulse holograms in two directions are recorded and then the reconstructed images through the entire volume of interest are stored in a computer by the image acquisition system. In the second stage, particles are separated from the background and the ROI-series images of one particle are combined along the optical axis. The three dimensional coordinates of this particle are determined using one of three auto-focusing parameters chosen on the basis of particle size. In the final third stage, the coordinate transform matrix obtained from two side single pulse holography is applied to achieve coordinate consistency.

Once the positions of individual particles have been obtained, the next step involves the application of the particle tracking algorithm to identify same particle pairs. Particle velocities are then calculated based on these pairings. Of the several algorithms used for this purpose, Baek and Lee

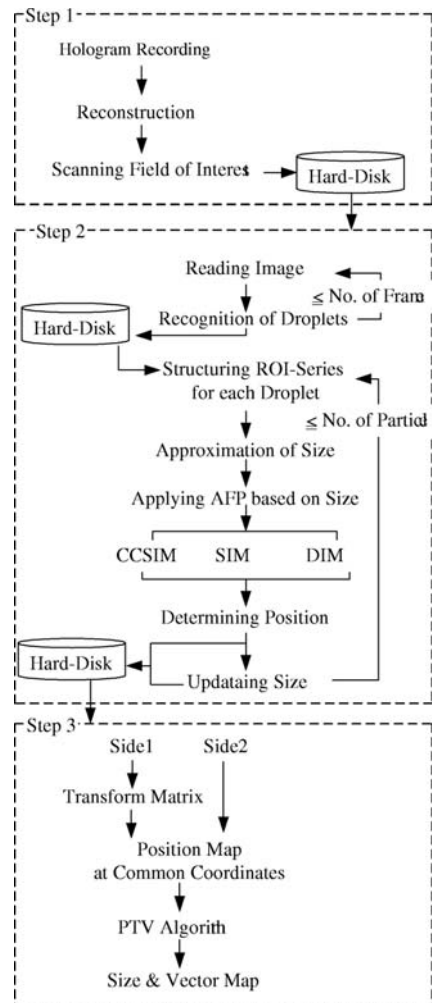


**Fig. 7** Flow chart for determination of sizes and velocities of particles

(1996)'s match probability algorithm was adopted in the present study, because it generates highly accurate pairing results, although the theory and the procedure involved are comparatively straightforward. The match probability algorithm repetitively evaluates the probability that particles are the same particles, and then particles showing the highest probability are paired. A more detailed description of this algorithm can be found in Baek and Lee (1996), Ballard and Brown (1982), and Lecuona et al. (2000).

### 4.2 Results of spray measurements

The measurement results of the sizes and 3-D

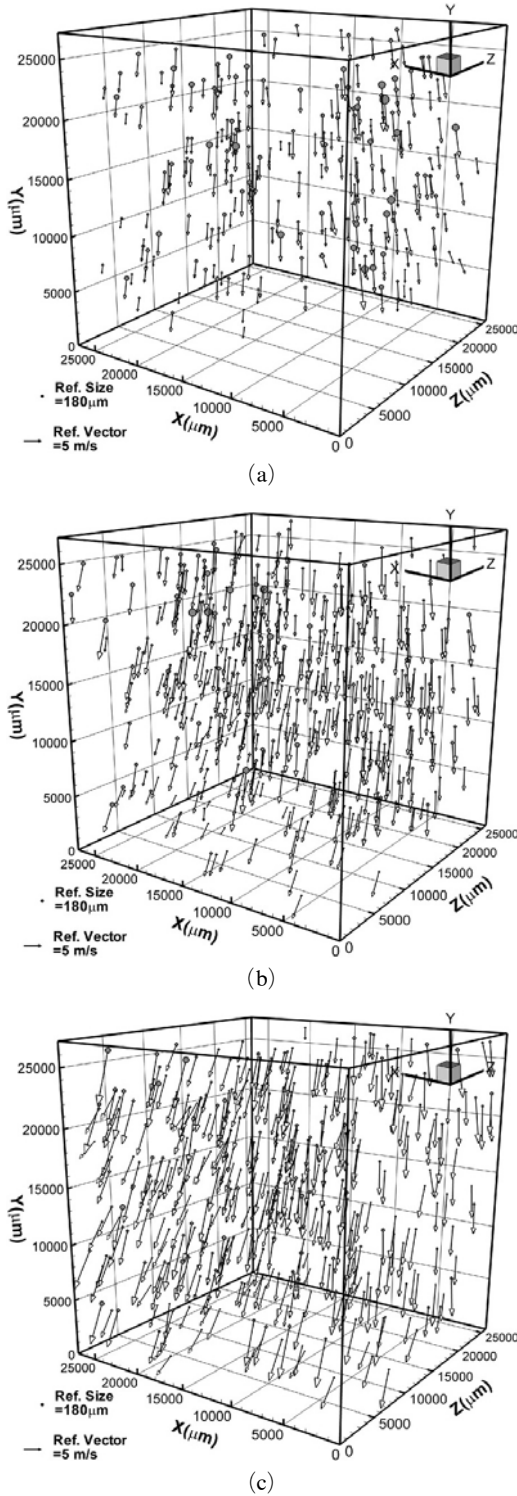


**Fig. 8** Measurement results of sizes and 3-D velocities of droplets ; (a)  $P=147$  kPa, (b)  $P=196$  kPa, (c)  $P=294$  kPa

velocities of droplets are shown in Fig. 8. As can be seen from the figure, droplet velocities show a typical behavior of droplet movements, i.e., radially outward and axially downward. The sizes and velocities of droplets become smaller and faster, respectively, as the injection pressure is increased.

The uncertainties in measurements of droplet velocities can be estimated from determination of three dimensional coordinates of particles. The uncertainty of a moved distance ( $R_i$ ) between two pulses in each direction,  $u_{Ri}$ , is related to the uncertainty of coordinate determination at single pulse,  $u_i$ .

$$u_{Ri} = \sqrt{2} u_i, \quad i = x, y, z \quad (1)$$

The components of particle velocity in each direction are calculated by dividing moved distance by the pulse interval,  $\Delta t$ , and thus the uncertainty of particle velocity in each direction is expressed as

$$\begin{aligned} u_{v_i} &= \sqrt{\left(\frac{\partial V_i}{\partial R_i} u_{Ri}\right)^2 + \left(\frac{\partial V_i}{\partial \Delta t} u_{\Delta t}\right)^2} \\ &= \sqrt{\left(\frac{1}{\Delta t} u_{Ri}\right)^2 + \left(\frac{R_i}{\Delta t^2} u_{\Delta t}\right)^2} \end{aligned} \quad (2)$$

The uncertainty of laser pulse interval,  $u_{\Delta t}$ , is zero. Therefore, the uncertainty of particle velocity in each direction simplifies to

$$u_{v_i} = \frac{u_{Ri}}{\Delta t} = \sqrt{2} \frac{u_i}{\Delta t} \quad (3)$$

The magnitude of particle velocity,  $V = \sqrt{V_x^2 + V_y^2 + V_z^2}$ , is obtained from the components of particle velocity so the uncertainty of particle velocity measured using the holographic method,  $u_v$ , is calculated from

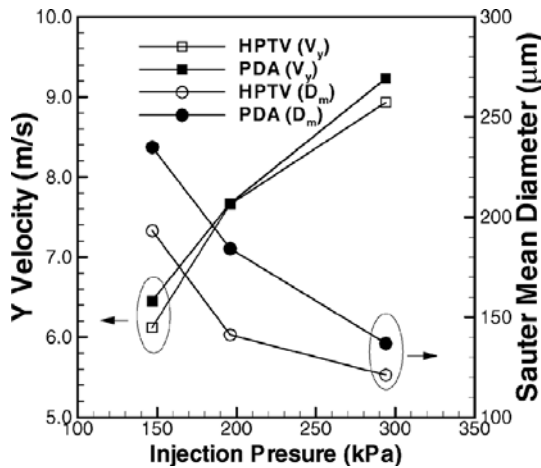
$$u_v = \sqrt{\left(\frac{\partial V}{\partial V_x} u_{v_x}\right)^2 + \left(\frac{\partial V}{\partial V_y} u_{v_y}\right)^2 + \left(\frac{\partial V}{\partial V_z} u_{v_z}\right)^2} \quad (4)$$

Table 2 shows magnitudes and components of particle velocities and their uncertainties calculated by Eqs. (3) and (4). In general, the uncertainties of particle velocity were much reduced in the present study as compared with the high uncertainties of conventional holographic techniques due to the long depth of focus in the optical axis.



**Table 2** Particle velocities and their uncertainties

$P$ [kPa]	$\Delta t$ [ $\mu$ s]	$V_x$ [m/s]	$V_y$ [m/s]	$V_z$ [m/s]	$V$ [m/s]	$u_{V_x}$ [m/s]	$u_{V_y}$ [m/s]	$u_{V_z}$ [m/s]	$u_V$ [m/s]
147	700	0.67	6.05	0.41	6.12	0.033	0.023	0.039	0.033
196	250	0.98	7.66	0.95	7.85	0.092	0.065	0.110	0.096
294	150	1.46	8.93	3.93	10.05	0.153	0.108	0.183	0.171

**Fig. 9** Comparison of holographic measurement results with those of PDPA

#### 4.3 Comparison with PDPA measurements

The measurement results of the sizes and three dimensional velocities of particles as determined by the developed holographic particle diagnostic system were compared with those obtained using a laser instrument, 2D-PDPA. The PDPA used in the present study was limited in terms of aspects like point and two dimensional velocity measurements. Measurement results were obtained by statistically analyzing data obtained for a large number samples. Therefore, in a sense it is inappropriate to compare holographic measurement results, which are based on an image processing technique, with those using PDPA. However, this type of comparison can be used to verify trends due to changes in experimental parameters. The comparison results are shown in Fig. 9. As the injection pressure was increased, both sets of results showed the same trend, i.e., droplet sizes and velocities became smaller and faster, respectively. The difference in droplet velocities between two methods is not big, but the results of particle size showed noticeable

differences, which were attributed to the small number of sample data examined using the holographic technique.

## 5. Conclusions

In this study, a diffused illumination holographic system to measure the quantitative features of particle fields like sizes and 3D velocities of moving particles was developed using an automatic image processing technique and the effectiveness of the developed system was demonstrated. The developed system adopts the unique methods such as auto-focusing parameters and size determination method. Firstly, orthogonal two-side optical systems for pulse laser recording, continuous laser reconstruction, and image acquisition were constructed. The developed system was validated by applying it to the volume of 2.5 mm<sup>3</sup> of droplet field produced by a commercial spray nozzle. Three dimensional positions of particles viewed in two normal directions were decided using auto-focusing parameters, and three dimensional particle velocities were extracted by the particle tracking algorithm. Finally, particle sizes and three dimensional velocities determined by the developed technique were compared with those by PDPA. Both results showed the same trend in sizes and velocities of spray droplets with small disagreement within acceptable range of errors. Based on this, we confirmed that the methods introduced in our previous research were effectively applied to the developed holographic particle diagnostic system for the analysis of particle field.

## References

Baek, S. J., 1997, *Development of Two-frame Particle Tracking Velocimetry System and its Ap-*

*plication to Turbulent Separated Flows*, Ph.D. Thesis, Pohang Univ. of Science and Technology.

Ballard, D. H. and Brown, C. M., 1982, *Computer Vision*, Prentice Hall, New Jersey, pp. 195~225.

Barnhart, D. H., Adrian, R. J. and Papen, G. C., 1994, "Phase-conjugate Holographic System for High-resolution Particle Image Velocimetry," *Applied Optics*, Vol. 33, pp. 7159~7170.

Choo, Y. J. and Kang, B. S., 2006, "The Characteristics of the Particle Position along an Optical Axis in Particle Holography," *Meas. Sci. Technol.*, Vol. 17, No. 4, pp. 761~770.

Feldmann, O., 1999, "Short-time Holography and Holographic PIV Applied to Engineering Problems," *Applied Optical Measurements*, Springer-Verlag, pp. 263~278.

Gonzalez, R. C., Woods, R. E. and Eddins, S. L., 2004, *Digital Image Processing using MATLAB*,

Pearson Education Inc., New Jersey, pp. 242~281.

Hausmann, G. and Lauterborn, W., 1980, "Determination of Size and Position of Fast Moving Gas Bubbles in Liquids by Digital 3-D Image Processing of Hologram Reconstructions," *Applied Optics*, Vol. 19, No. 20, pp. 3529~3535.

Kang, B. S., 1995, *A Holographic Study of the Dense Region of a Spray Created by Two Impinging Jets*, Ph.D. Thesis, Univ. of Illinois, Chicago.

Lecuona, A., Rodriguez, P. A. and Zequeire, R. I., 2000, "Volumetric Characterization of Dispersed Two-phase Flows by Digital Image Analysis," *Meas. Sci. Technol.*, Vol. 11, pp. 1152~1161.

Vikram, C. S., 1979, *Particle Field Holography*, Cambridge University Press.